Eurasia Specialized Veterinary Publication

International Journal of Veterinary Research and Allied Science
ISSN:3062-357X

2022, Volume 2, Issue 2, Page No: 63-72

Available online at: www.esvpub.com/

Semi-Quantitative Detection of PRRSV-1 RNA in Pig Lungs Using RNAscope and QuPath-Based Image Analysis

Mia Lopez[1], Daniel Gonzalez[1*], Charlotte Wilson[1]

[1]Department of Population Health and Pathobiology, College of Veterinary Medicine, North Carolina State University, Raleigh, NC, United States.

***E-mail** ✉ dgonzalez@mail.com

ABSTRACT

The viruses Betaarterivirus suid 1 and Betaarterivirus suid 2 are recognized as the etiological agents of porcine reproductive and respiratory syndrome (PRRS), a condition that severely impacts swine health and inflicts major economic damage across leading pig-producing nations. In this study, we describe the establishment of an innovative RNA in situ hybridization method (RNAscope) tailored for the visualization of PRRS virus (PRRSV) RNA in the lung tissues of experimentally infected pigs. Lung samples from 20 piglets inoculated with a wild-type, highly virulent PRRSV-1 isolate were analyzed using this approach. To assess whether RNAscope could be used in a semi-quantitative manner, the proportion of infected cells determined by digital image analysis (QuPath) was compared with viral RNA levels measured by real-time quantitative reverse transcription polymerase chain reaction (qRT-PCR) conducted on the same samples. A strong correspondence between both molecular results was observed (pseudo $R^2 = 0.3894$, $p = 0.004$). This study represents the first demonstration of RNAscope's application for detecting PRRSV-1 in an experimental infection model.

Keywords: Porcine reproductive, Respiratory syndrome virus, RNAscope in situ hybridization, qRT-PCR, QuPath

Received: 09 January 2022
Revised: 11 March 2022
Accepted: 11 March 2022

How to Cite This Article: Lopez M, Gonzalez D, Wilson C. Semi-Quantitative Detection of PRRSV-1 RNA in Pig Lungs Using RNAscope and QuPath-Based Image Analysis. Int J Vet Res Allied Sci. 2022;2(1):63-72. https://doi.org/10.51847/TxSWiwqFZ0

Introduction

Porcine reproductive and respiratory syndrome (PRRS) remains one of the most prevalent and economically detrimental viral diseases affecting pig populations globally [1, 2]. The causative agent, PRRS virus (PRRSV), encompasses two viral species—*Betaarterivirus suid 1* and *Betaarterivirus suid 2*—classified under the genus *Betaarterivirus* of the *Arteriviridae* family within the order *Nidovirales* [3]. The virus exhibits exceptional genetic heterogeneity, both within and between these two species [4, 5]. PRRSV shows a distinct tropism for pulmonary tissue, replicating primarily within alveolar macrophages, although it has also been located in intravascular and interstitial macrophage populations [6–9]. The membrane protein CD163, functioning as a hemoglobin–haptoglobin receptor, has been identified as the key determinant for viral attachment and entry. Notably, animals genetically engineered to lack CD163—either completely or only at the virus-binding domain—exhibit full resistance to infection [10, 11].

Clinically, PRRS manifests in a broad range of forms, from mild or inapparent infections to acute systemic illness characterized by high fever, hemorrhages, and elevated mortality. In breeding herds, reproductive disturbances such as abortion, premature farrowing, and stillbirth are common, while surviving neonates often show low birth weight and weak vitality. Infected juveniles and finishing pigs frequently experience respiratory distress, and in males, the infection can lead to reduced semen quality [12, 13].

Reverse transcription polymerase chain reaction (RT-PCR) is the predominant laboratory tool for direct PRRSV detection, and viral quantification is typically performed by real-time qPCR. Nevertheless, the high sequence variability among strains can compromise test sensitivity [14, 15]. Virus localization in tissues may be achieved through immunohistochemistry (IHC), fluorescent antibody (FA) staining, or in situ hybridization (ISH), which target either viral proteins or nucleic acids. Unlike PCR, these approaches provide spatial context by visualizing the pathogen within lesions. However, their sensitivity tends to be lower, often affected by autolysis, suboptimal fixation, or genetic and antigenic variation in the virus. For PRRSV, detection of the nucleocapsid (N) or glycoprotein 5 (GP5) antigens can be carried out on formalin-fixed paraffin-embedded (FFPE) sections using chromogenic IHC or on frozen tissues with FA staining, though these assays are generally less sensitive than nucleic acid–based detection [16]. The limited performance is primarily due to pronounced antigenic diversity among circulating isolates and the small number of commercially available antibodies.

In situ hybridization methods use complementary probes to detect specific nucleic acid sequences of a pathogen. These probes are typically tagged with digoxigenin, biotin, or dinitrophenol (DNP). Traditional ISH assays relying on short oligonucleotide probes are often less sensitive than riboprobes, owing to smaller hybridization targets and weaker labeling efficiency [17]. Larochelle and colleagues described an ISH technique employing digoxigenin-labeled cDNA probes for detecting PRRSV in both cultured cells and FFPE tissues, demonstrating that this method can serve as a sensitive and specific diagnostic tool as well as a valuable resource for pathogenesis studies [18].

A recently introduced RNA-based ISH platform (RNAscope®, Advanced Cell Diagnostics Inc., Biotechne, Abingdon, UK) offers a more advanced alternative. It employs pairs of 18–25-base Z-shaped probes that bind in close proximity on the target RNA sequence. A visible chromogenic or fluorescent signal is generated only when both probes hybridize adjacently, allowing the attachment of an amplifier probe that enhances signal strength. This design confers superior sensitivity and specificity, as hybridization of as few as three probe pairs can yield a detectable signal. Because each probe targets a short RNA fragment, RNAscope can also detect partially degraded RNA molecules [19–21]. These attributes make the assay suitable for samples with moderate decomposition and less susceptible to the effects of genetic variation compared with classical ISH using single linear probes. RNAscope has already been employed to identify several porcine viruses, including Seneca Valley virus [22], a neuroinvasive astrovirus [23], and PCV3 [24]; our group has also successfully utilized it for detecting atypical porcine pestivirus [25].

Digital slide generation and computer-assisted image analysis have become standard practices in both research and diagnostic pathology for humans. These programs enable automated and objective evaluation of stained tissue samples, including precise quantification of cell numbers and staining intensity. Such tools provide an efficient alternative to manual cell counting, which is often labor-intensive, difficult to reproduce, and subject to considerable variability between observers [26].

The primary purpose of the current study was to establish an in situ hybridization (ISH) protocol capable of identifying PRRSV in lung tissues collected from young pigs experimentally infected with a highly virulent PRRSV-1 strain. A secondary goal was to apply digital analysis for ISH-positive cell quantification and to compare those data with histopathological pneumonia severity scores and quantitative RT-PCR findings obtained from corresponding lung lobes.

Materials and Methods

Animal ethics approval

All experimental procedures complied with existing Hungarian legislation on animal research and welfare. The study was conducted under the ethical authorization number BA02/2000-43/2017.

Sample collection

A total of 25 pigs, each seven weeks old, were used in this investigation. Of these, 20 were intranasally challenged with 2.5 mL of cell culture supernatant containing 10^6 $TCID_{50}$ of the highly virulent PRRSV-1 Austrian field strain AUT15-33 (also known as “ACRO”) [27]. The remaining five animals were mock-inoculated and served as uninfected controls. All animals were humanely euthanized at 14 days post-infection (DPI), corresponding to nine weeks of age. During necropsy, all major organs were examined, and each pulmonary lobe was collected and placed into 10% neutral buffered formaldehyde (NBF) for subsequent histopathological and ISH evaluation.

Matched samples from the same lobes were submitted to the University of Veterinary Medicine, Vienna, for quantitative assessment of PRRSV RNA.

Tissue preparation and conventional histopathology

After 24 hours of fixation in NBF at ambient temperature, tissues were trimmed and passed through graded ethanol and xylene steps using an automated tissue processor. The processed samples were then embedded in paraffin, sectioned manually at 4 µm thickness, and mounted on Superfrost+ adhesion slides (Thermo Fisher Scientific, Waltham, MA, USA).

For histology, slides were deparaffinized and rehydrated through xylene and alcohol series, respectively, followed by routine hematoxylin and eosin staining carried out in an automated stainer. Lung lesions were evaluated according to the scoring system described by Balka *et al*. [28]. The following pathological changes were recorded: (1) pneumocyte enlargement and proliferation, (2) septal infiltration with mononuclear cells, (3) intra-alveolar necrotic material, (4) inflammatory cell accumulation in alveolar spaces, and (5) perivascular inflammatory infiltration. Each alteration was scored for both severity (0–3) and distribution (0–3) in all seven lobes. Lobar scores were summed to provide individual and total lung severity indices, with maximum possible scores of 30 per lobe and 210 for the whole lung.

RNA in situ hybridization (RNAscope)

The virus-specific RNAscope probe (Cat. No. 519571) was designed based on the AUT15-33 genome sequence (Accession No. MT000052.1), targeting the ORF7 gene. A probe detecting the housekeeping gene *peptidyl-prolyl isomerase B* (Sus scrofa–PPIB, Cat. No. 428591) served as a positive control, whereas bacterial *dihydropicolinate reductase* (DapB, Cat. No. 310043) was used as a negative control.

ISH was performed on sections from the left medial lung lobe to minimize variability due to uneven lesion distribution (cranial and middle lobes consistently showed more pronounced changes than caudal ones). The assay followed the manufacturer's standard protocol. Briefly, endogenous peroxidase activity was quenched, and sections were subjected to heat-induced target retrieval in 1× Target Retrieval solution for 15 minutes. After rinsing twice with distilled water and once with 96% ethanol, slides were air-dried. RNAscope® Protease Plus reagent was then applied, and slides were incubated for 30 minutes at 40 °C in a HybEZ™ hybridization oven (Advanced Cell Diagnostics, Newark, CA, USA).

Next, 200 µL of the designated hybridization probe mixture was added to each sample, followed by a 2-hour incubation at 40 °C. After two 2-minute washes in 1× wash buffer at room temperature, amplification reagents (Amp 1–6) were sequentially applied as instructed.

Signal development was achieved by adding approximately 120 µL of a 1:60 Fast RED-B to Fast RED-A solution and incubating for 10 minutes in the hybridization chamber at room temperature. Slides were rinsed in distilled water, counterstained with Gill No. 2 hematoxylin (Merck, Darmstadt, Germany) for 2 minutes, and then washed twice with distilled water. They were briefly immersed in 0.02% ammonia water for 10 seconds, washed again, and air-dried at 60 °C for 15–25 minutes. Finally, slides were cleared in xylene, mounted with EcoMount medium, and covered with glass coverslips.

Tissue scanning and digital analysis

For each piglet, a single sample from the left medial lung lobe prepared via the RNAscope procedure was imaged and digitized using a Pannoramic Midi slide scanner (3D Histech, Budapest, Hungary). Representative digital slides were visualized through SlideViewer (3D Histech) and further processed using QuPath software (version 0.1.2, qupath.github.io) [29]. The proportion of PRRSV-positive cells was assessed within zones that reflected the overall histological profile. Each analyzed slide contained annotated areas totaling 2.37 mm², equivalent to 10 high-power microscopic fields (HPFs). The "positive cell detection" function within the "analyze → cell detection" menu was employed, and quantitative data were obtained through the "show detection measurements" option under the "measure" tab. The software automatically reported both total and positive cell counts along with their relative percentages. A complete analytical workflow is described in the Supplementary Material.

Quantification of PRRSV RNA (qRT-PCR)

Portions of lung tissue (50 mg) were homogenized using the TissueLyser II system (Qiagen GmbH, Hilden, Germany) for 3 min. Following homogenization, samples were vortexed, centrifuged to separate phases, and 200

µL of the supernatant was used for RNA extraction in the QiaCubeHT automated platform with the Cador Pathogen Kit (Qiagen GmbH), following the manufacturer's guidelines.

Two microliters of purified RNA served as the template for ORF7-targeted amplification using the Luna OneStep RT-PCR Kit (NEB). The specific primer set consisted of forward primer TCAACTGTGCCAGTTGCTGG, reverse primer TGRGGCTTCTCAGGCTTTTC, and a labeled probe 5'Fam-CCCAGCGYCRRCARCCTAGGG Tamra-3'. The oligonucleotide sequences were adapted from Egli *et al*. [30] to match the PRRSV-1 AUT15-33 strain sequence.

Absolute genome copy quantification (GE) was determined using a dilution series of SP6-transcribed RNA derived from cloned AUT15-33 cDNA (4872 nt). RNA was produced by SP6 polymerase transcription from an AclI-linearized plasmid (pLS69), followed by DNAse I (NEB) treatment and RNA purification using the RNeasy Kit (Qiagen GmbH, Germany). Concentrations were measured via a Quantus fluorometer with an RNA-selective dye (Promega GmbH, Walldorf, Germany). Genome copy numbers were calculated using the algorithm from http://scienceprimer.com/copy-number-calculator-for-realtime-pcr [31] and validated through droplet digital PCR (Applied Biosystems, Thermo Fisher Scientific, Waltham, MA, USA). Quantitative PCR reactions were performed on an Applied Biosystem 7300 platform (Thermo Fisher Scientific).

Statistical evaluation

Associations between the proportion of PRRSV-infected cells (RNAscope ISH) and (1) the log10 genome copy counts from qPCR, (2) the lesion severity score within the same lobe, and (3) the total lung pathology grade were analyzed using beta regression with a logit link. Modeling was carried out in R version 4.0.3 [1] employing the *betareg* package [2]. A p-value ≤ 0.05 indicated statistical significance.

Results and Discussion

Histopathological assessment and in situ hybridization

Marked disparities in lesion scores were noted between the infected and control animals (data not displayed, as quantitative lesion analysis was beyond the study scope).

As shown in **Figure 1**, slides hybridized with *Sus scrofa* PPIB probes displayed uniform, bright cytoplasmic red signals, confirming adequate fixation and RNA preservation. In contrast, slides treated with DapB negative control probes lacked visible staining, verifying the specificity of the method.

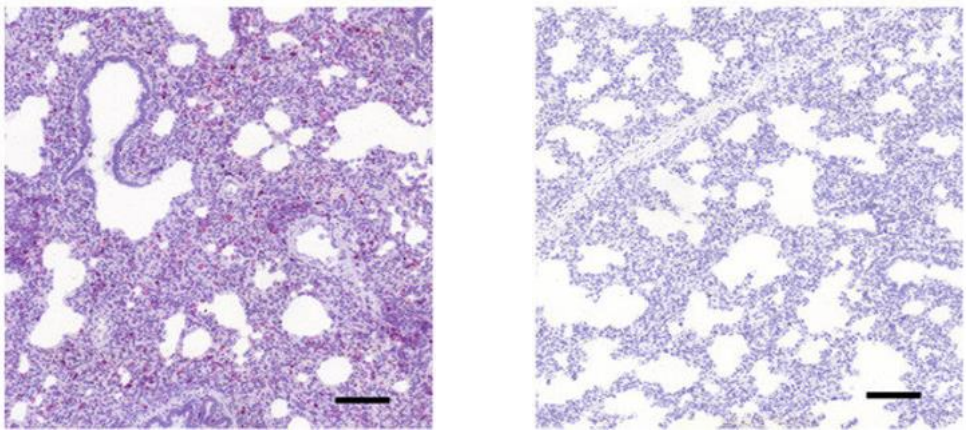

a) b)

Figure 1. Representative lung tissue showing positive control (a, PPIB-labeled) and negative control (b, DapB-labeled) RNAscope slides (12×; scale bar = 100 µm).

Figures 2–4 illustrate multifocal PRRSV genome localization as scattered or merging red puncta within the lungs of infected pigs. Positively stained cells, mainly macrophages and alveolar epithelial cells, were irregularly distributed, frequently concentrated in areas with more pronounced inflammation and thickened intralobular septa. The highest density of PRRSV-positive cells appeared in interalveolar and intralobular septal regions.

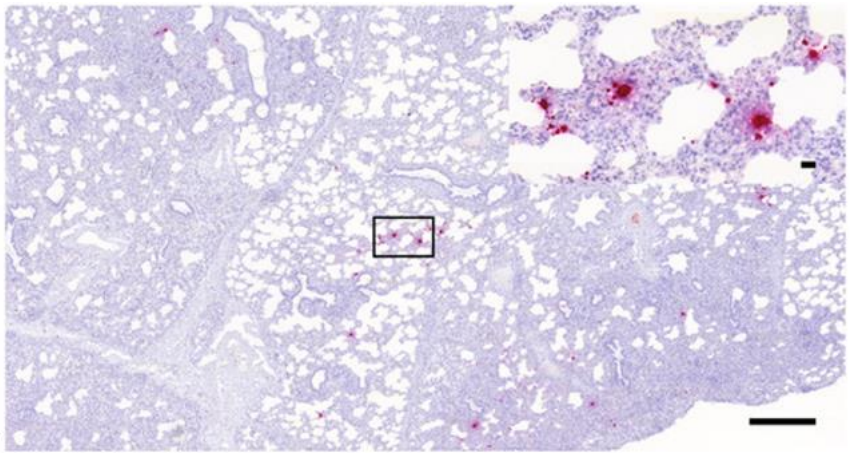

Figure 2. Porcine lung section showing sparse PRRSV-positive cells (RNAscope ISH, 3×; bar = 500 µm). Inset: magnified view (40×; bar = 20 µm).

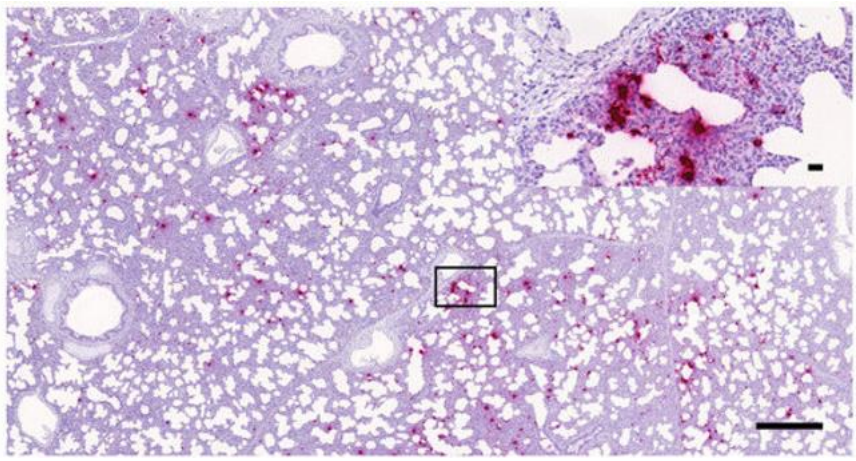

Figure 3. Lung tissue with moderate PRRSV infection (RNAscope ISH, 3×; bar = 500 µm). Inset: higher magnification (40×; bar = 20 µm).

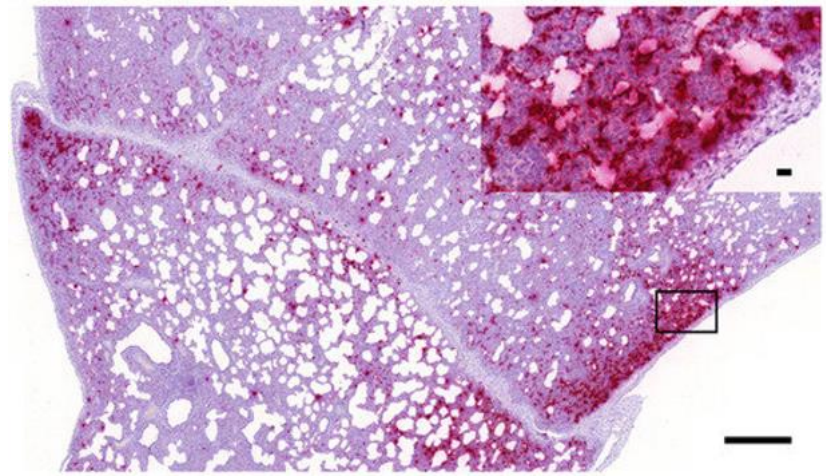

Figure 4. Lung sample with extensive PRRSV-positive cell presence (RNAscope ISH, 3×; bar = 500 µm). Inset: detailed view (40×; bar = 20 µm).

qRT-PCR

As anticipated, PCR assays yielded no detectable amplification in lung tissues obtained from the uninfected control group. In contrast, every animal inoculated with strain AUT15-33 tested positive for viral genomic RNA

within lung samples. The quantitative data, expressed as log_{10} genome copies per gram of tissue, are presented in **Table 1**, ranging between 8.18 and 11.68 for the infected group.

Table 1. Percentage of PRRSV-positive cells correlated with the base-10 logarithm of genome copies per gram of lung tissue.

Animal ID	Fraction of Infected Cells (%)	log_{10} Genome Copies per gram	Lung Median Severity[a]	Total Severity[b]
19	0.00	0.00	0	0
9	0.00	0.00	0	0
7	0.00	0.00	0	0
4	0.00	0.00	0	0
2	0.00	0.00	0	0
23	0.16	10.09	17	68
22	0.19	10.95	20	143
14	0.20	8.79	10	72
25	0.41	9.80	12	67
21	0.72	9.71	17	101
20	1.04	10.41	16	77
17	1.04	8.18	12	56
5	1.86	10.65	26	180
6	1.88	10.68	19	157
12	2.73	11.46	20	135
3	2.93	10.98	17	101
18	3.86	10.73	23	139
13	3.97	10.66	12	65
1	4.24	11.25	17	107
15	4.29	10.91	21	115
11	5.60	11.00	11	110
24	5.79	10.70	25	144
8	8.25	10.93	19	110
10	9.02	10.99	20	136
16	26.70	11.68	21	137

a: Severity and distribution indices for the left medial lobe.

b: Combined severity and distribution scores across all pulmonary lobes.

Digital image evaluation

Following the digitization of RNAscope-treated lung sections, image processing was performed using QuPath software to determine total and infected cell counts. As expected, no PRRSV-positive cells were found in control samples. Among the infected pigs, the percentage of labeled cells varied considerably between individuals, ranging from 0.16% to 26.7% within annotated tissue regions, as detailed in **Table 1**.

Beta regression analysis

Three beta regression models were developed to examine the association between the proportion of RNAscope ISH-positive cells and three explanatory parameters:

(1) overall histological severity and lesion distribution across all seven lobes, (2) severity and distribution scores specific to the left medial lobe, and (3) log_{10} genome copy numbers determined by qPCR in the same lobe.

A statistically significant relationship emerged between the fraction of infected cells and the qPCR-derived log_{10} genome copies in the corresponding lobe (pseudo $R^2 = 0.3894$, $p = 0.004$). However, neither the overall histological severity (pseudo $R^2 = 0.1664$, $p = 0.1806$) nor the severity within the left medial lobe (pseudo $R^2 = 0.1354$, $p = 0.1455$) showed significant correlation with ISH labeling intensity.

Discussion

Routine detection of PRRSV primarily relies on RT-PCR, whereas visualization of viral antigen via immunohistochemistry (IHC) or genome localization using in situ hybridization (ISH) is rarely included in

standard diagnostic workflows. These microscopic techniques, widely applied in both veterinary and human pathology, enable simultaneous evaluation of lesion morphology, viral load, spatial distribution, and cellular tropism of the pathogen within tissues. Such approaches are valuable for clarifying the pathological involvement of PRRSV in naturally occurring respiratory syndromes in swine [32], though they are most often implemented under controlled experimental conditions involving single-agent infection [33].

Nevertheless, the detection of viruses in histological slides through IHC poses several technical challenges. The reliability of staining outcomes depends heavily on preanalytical variables such as fixative concentration and pH, the interval between necropsy and fixation (which affects autolysis), and fixation duration. These factors often vary in samples submitted for routine diagnostics, where procedural quality control is less standardized compared with human pathology [34]. Combined with the pronounced genetic and antigenic diversity of PRRSV strains, these issues render IHC-based antigen detection less sensitive than RNA-targeting molecular methods [16].

A variety of RNA-specific ISH platforms have been developed for PRRSV, including fluorescence-based (FISH), chromogenic (CISH), and tyramide signal amplification (TISH) systems [32, 35]. In this study, the newly optimized RNAscope ISH protocol, designed against the ORF7 genomic sequence of the PRRSV-1 AUT15-33 strain, successfully demonstrated viral presence in the lungs of experimentally infected pigs. Proper fixation with 10% neutral buffered formalin and adequate fixation duration preserved RNA integrity and tissue structure. Prior literature documents the use of RNAscope primarily for PRRSV-2 strains [36, 37]; thus, this work extends its validated use to PRRSV-1.

The detected distribution pattern of viral RNA closely paralleled the severity of interstitial pneumonia—regions with stronger inflammatory responses generally contained higher concentrations of viral signal. Nonetheless, statistical analysis revealed no significant relationship between the fraction of ISH-positive cells and either the lesion severity in the left medial lobe or the overall lung score. The heterogeneity of lesion severity among individuals likely reduced statistical power, implying that examination of a larger number of lung sections may be required to detect a meaningful association.

In order to assess the assay's potential for quantitative evaluation, we first applied automated, software-assisted positive cell counting on digitized tissue sections scanned using a slide-scanning system. Computerized quantification methods are widely adopted in diagnostic pathology—particularly for analyses such as Ki67 proliferation indices and tumor-infiltrating lymphocyte enumeration—and have been demonstrated to deliver accuracy and reproducibility comparable to, or occasionally surpassing, traditional manual counting approaches [26, 38, 39].

A significant correlation was observed between the proportion of PRRSV-positive cells and the $\log_{10}$-transformed genome copy numbers determined by qPCR from the same pulmonary lobe. The discrepancy between elevated genome copy counts and relatively low proportions of labeled cells in certain specimens can likely be attributed to uneven lesion distribution and ISH signal heterogeneity, as well as to the two-dimensional nature of ISH analysis compared with qPCR, which measures total RNA from the entire tissue fragment.

These findings demonstrate that RNAscope ISH, when followed by digital image-based quantification, provides a robust means to evaluate viral load directly within histological architecture. From a pathological perspective, this localized visualization of viral presence is of greater interpretative value than bulk PCR results, since it permits direct correlation of viral signal with lesion morphology and spatial context.

Although the RNAscope technique and subsequent image analysis remain relatively costly and labor-intensive, limiting their use in day-to-day diagnostic workflows, the study highlights their potential as high-value tools for experimental infection research and vaccine efficacy testing. In such trials, reductions in pulmonary inflammation accompanied by decreased counts of infected cells can serve as critical efficacy indicators.

Looking ahead, our objective is to validate the assay using diverse PRRSV-positive FFPE samples. Since the probes target one of the most conserved regions of the viral genome (ORF7) and the technology employs numerous short, highly sensitive probe pairs, it is highly probable that this method can also be applied to detect other PRRSV genotypes. The inclusion of both a housekeeping gene probe (positive control) and a bacterial probe (negative control) offers additional quality assurance, enabling verification of RNA preservation and fixation quality in FFPE blocks of unknown processing history—key determinants for obtaining reliable RNAscope signals, particularly when using 10% neutral buffered formalin (NBF).

Conclusion

Through implementation of the novel RNAscope ISH assay, we successfully identified and localized PRRSV-1 in the lung tissues of pigs experimentally challenged with the AUT15-33 strain. Digital image-derived positive cell counts, when statistically compared with the $\log_{10}$ genome copy numbers measured by qPCR from matching lobes, exhibited a strong and significant association. Collectively, these results confirm that RNAscope ISH combined with computerized image analysis offers valuable semi-quantitative insight into PRRSV infection dynamics in situ, providing both molecular precision and histopathological context.

Acknowledgments: None

Conflict of Interest: None

Financial Support: None

Ethics Statement: None

References

1. Holtkamp DJ, Kliebenstein JB, Neumann EJ, Zimmerman JJ, Rotto HF, Yoder TK, et al. Assessment of the economic impact of porcine reproductive and respiratory syndrome virus on United States pork producers. J Swine Health Prod. 2013 Mar-Apr;21(2):72-84.
2. Lunney JK, Benfield DA, Rowland RR. Porcine reproductive and respiratory syndrome virus: an update on an emerging and re-emerging viral disease of swine. Virus Res. 2010 Dec;154(1-2):1-6.
3. Sánchez-Carvajal JM, Rodríguez-Gómez IM, Ruedas-Torres I, Larenas-Muñoz F, Díaz I, Revilla C, et al. Activation of pro- and anti-inflammatory responses in lung tissue injury during the acute phase of PRRSV-1 infection with the virulent strain Lena. Vet Microbiol [Internet]. 2020 Jul [cited 2025 Nov 12];246:108744.
4. Balka G, Podgórska K, Brar MS, Bálint Á, Cadar D, Celer V, et al. Genetic diversity of PRRSV 1 in Central Eastern Europe in 1994–2014: origin and evolution of the400 virus in the region. Sci Rep [Internet]. 2018 May [cited 2025 Nov 12];8:7811.
5. Shi M, Lam TT, Hon CC, Hui RK, Faaberg KS, Wennblom T, et al. Molecular epidemiology of PRRSV: a phylogenetic perspective. Virus Res. 2010 Dec;154(1-2):7-17.
6. Bordet E, Maisonnasse P, Renson P, Bouguyon E, Crisci E, Tiret M, et al. Porcine alveolar macrophage-like cells are pro-inflammatory pulmonary intravascular macrophages that produce large titers of porcine reproductive and respiratory syndrome virus. Sci Rep [Internet]. 2018 Jul [cited 2025 Nov 12];8:10172.
7. Gómez-Laguna J, Salguero FJ, Barranco I, Pallarés FJ, Rodríguez-Gómez IM, Bernabé A, et al. Cytokine expression by macrophages in the lung of pigs infected with the porcine reproductive and respiratory syndrome virus. J Comp Pathol. 2010 Jan;142(1):51-60.
8. Lunney JK, Fang Y, Ladinig A, Chen N, Li Y, Rowland B, et al. Porcine reproductive and respiratory syndrome virus (PRRSV): pathogenesis and interaction with the immune system. Annu Rev Anim Biosci. 2016 Feb;4:129-54.
9. Nauwynck HJ, Van Gorp H, Vanhee M, Karniychuk U, Geldhof M, Cao A, et al. Micro-dissecting the pathogenesis and immune response of PRRSV infection paves the way for more efficient PRRSV vaccines. Transbound Emerg Dis. 2012 Feb;59 Suppl 1:50-4.
10. Burkard C, Opriessnig T, Mileham AJ, Stadejek T, Ait-Ali T, Lillico SG, et al. Pigs lacking the scavenger receptor cysteine-rich domain 5 of CD163 are resistant to porcine reproductive and respiratory syndrome virus 1 infection. J Virol [Internet]. 2018 Jun [cited 2025 Nov 12];92(12):e00415-18.
11. Whitworth KM, Rowland RR, Ewen CL, Trible BR, Kerrigan MA, Cino-Ozuna AG, et al. Gene-edited pigs are protected from porcine reproductive and respiratory syndrome virus. Nat Biotechnol. 2016 Jan;34(1):20-2.
12. Rossow KD. Porcine reproductive and respiratory syndrome. Vet Pathol. 1998 Jan;35(1):1-20.
13. Schulze M, Revilla-Fernández S, Schmoll F, Grossfeld R, Griessler A. Effects on boar semen quality after infection with porcine reproductive and respiratory syndrome virus: a case report. Acta Vet Scand [Internet]. 2013 Feb [cited 2025 Nov 12];55:16.

14. Balka G, Hornyák A, Bálint A, Benyeda Z, Rusvai M. Development of a one-step real-time quantitative PCR assay based on primer-probe energy transfer for the detection of porcine reproductive and respiratory syndrome virus. J Virol Methods. 2009 Jun;158(1-2):41-5.
15. Toplak I, Rihtarič D, Hostnik P, Grom J, Stukelj M, Valenčak Z. Identification of a genetically diverse sequence of porcine reproductive and respiratory syndrome virus in Slovenia and the impact on the sensitivity of four molecular tests. J Virol Methods. 2012 Jan;179(1):51-6.
16. Zimmerman JJ, Dee SA, Holtkamp DJ, Murtaugh MP, Stadejek T, Stevenson GW, et al. Porcine reproductive and respiratory syndrome viruses (porcine arteriviruses). In: Zimmerman JJ, Karriker LA, Ramirez A, Schwartz KJ, Stevenson GW, Zhang J, editors. Diseases of swine. 11th ed. Hoboken (NJ): Wiley Blackwell; 2018. p. 696-7.
17. Maes RK, Langohr IM, Wise AG, Smedley RC, Thaiwong T, Kiupel M. Beyond H&E: integration of nucleic acid-based analyses into diagnostic pathology. Vet Pathol. 2014 Jan;51(1):238-56.
18. Larochelle R, Mardassi H, Dea S, Magar R. Detection of porcine reproductive and respiratory syndrome virus in cell cultures and formalin-fixed tissues by in situ hybridization using a digoxigenin-labeled probe. J Vet Diagn Invest. 1996 Jan;8(1):3-10.
19. Bingham V, McIlreavey L, Greene C, O'Doherty E, Clarke R, Craig S, et al. RNAscope in situ hybridization confirms mRNA integrity in formalin-fixed, paraffin-embedded cancer tissue samples. Oncotarget [Internet]. 2017 Nov [cited 2025 Nov 12];8(55):93392-403.
20. Wang F, Flanagan J, Su N, Wang LC, Bui S, Nielson A, et al. RNAscope: a novel in situ RNA analysis platform for formalin-fixed, paraffin-embedded tissues. J Mol Diagn. 2012 Jan;14(1):22-9.
21. Wang H, Wang MX, Su N, Wang LC, Wu X, Bui S, et al. RNAscope for in situ detection of transcriptionally active human papillomavirus in head and neck squamous cell carcinoma. J Vis Exp [Internet]. 2014 Mar [cited 2025 Nov 12];(85):51426.
22. Resende TP, Marthaler DG, Vannucci FA. A novel RNA-based in situ hybridization to detect Seneca Valley virus in neonatal piglets and sows affected with vesicular disease. PLoS ONE [Internet]. 2017 Mar [cited 2025 Nov 12];12(3):e0173190.
23. Boros Á, Albert M, Pankovics P, Bíró H, Pesavento PA, Phan TG, et al. Outbreaks of neuroinvasive astrovirus associated with encephalomyelitis, weakness, and paralysis among weaned pigs, Hungary. Emerg Infect Dis. 2017 Dec;23(12):1982-93.
24. Arruda B, Piñeyro P, Derscheid R, Hause B, Byers E, Dion K, et al. PCV3-associated disease in the United States swine herd. Emerg Microbes Infect [Internet]. 2019 [cited 2025 Nov 12];8(1):684-98.
25. Dénes L, Ruedas-Torres I, Szilasi A, Balka G. Detection and localization of atypical porcine pestivirus in the testicles of naturally infected, CT-affected piglets. Transbound Emerg Dis [Internet]. 2021 [cited 2025 Nov 12].
26. Stålhammar G, Robertson S, Wedlund L, Lippert M, Rantalainen M, Bergh J, et al. Digital image analysis of Ki67 in hot spots is superior to both manual Ki67 and mitotic counts in breast cancer. Histopathology. 2018 Jun;72(6):974-89.
27. Sinn LJ, Klingler E, Lamp B, Brunthaler R, Weissenböck H, Rümenapf T, et al. Emergence of a virulent porcine reproductive and respiratory syndrome virus (PRRSV) 1 strain in Lower Austria. Porcine Health Manag [Internet]. 2016 Nov [cited 2025 Nov 12];2:28.
28. Balka G, Ladinig A, Ritzmann M, Saalmüller A, Gerner W, Käser T, et al. Immunohistochemical characterization of type II pneumocyte proliferation after challenge with type I porcine reproductive and respiratory syndrome virus. J Comp Pathol. 2013 Aug-Oct;149(2-3):322-30.
29. Bankhead P, Loughrey MB, Fernández JA, Dombrowski Y, McArt DG, Dunne PD, et al. QuPath: open source software for digital pathology image analysis. Sci Rep [Internet]. 2017 Dec [cited 2025 Nov 12];7:16878.
30. Egli C, Thür B, Liu L, Hofmann MA. Quantitative TaqMan RT-PCR for the detection and differentiation of European and North American strains of porcine reproductive and respiratory syndrome virus. J Virol Methods. 2001 Oct;98(1):63-75.
31. Staroscik A. Science Primer [Internet]. [cited 2025 Nov 12]. Available from: http://scienceprimer.com/copy-number-calculator-for-realtime-pcr
32. Han K, Seo HW, Oh Y, Kang I, Park C, Kang SH, et al. Evaluation of monoclonal antibody-based immunohistochemistry for the detection of European and North American porcine reproductive and

respiratory syndrome virus and a comparison with in situ hybridization and reverse transcription polymerase chain reaction. J Vet Diagn Invest. 2012 Jul;24(4):719-24.

33. Sánchez-Carvajal JM, Ruedas-Torres I, Carrasco L, Pallarés FJ, Mateu E, Rodríguez-Gómez IM, et al. Activation of regulated cell death in the lung of piglets infected with virulent PRRSV-1 Lena strain occurs earlier and mediated by cleaved Caspase-8. Vet Res [Internet]. 2021 Jan [cited 2025 Nov 12];52:12.
34. Van Alstine WG, Popielarczyk M, Albregts SR. Effect of formalin fixation on the immunohistochemical detection of PRRS virus antigen in experimentally and naturally infected pigs. J Vet Diagn Invest. 2002 Nov;14(6):504-7.
35. Trang NT, Hirai T, Ngan PH, Lan NT, Fuke N, Toyama K, et al. Enhanced detection of porcine reproductive and respiratory syndrome virus in fixed tissues by in situ hybridization following tyramide signal amplification. J Vet Diagn Invest. 2015 May;27(3):326-31.
36. Cui MM, Li JN, Wang G, He XJ, Weng CJ. Detection of porcine reproductive and respiratory syndrome virus RNA using RNAscope in situ hybridization. Chin J Prev Vet Med. 2018;40(6):596-600.
37. Song J, Gao P, Kong C, Zhou L, Ge X, Guo X, et al. The nsp2 hypervariable region of porcine reproductive and respiratory syndrome virus strain JXwn06 is associated with viral cellular tropism to primary porcine alveolar macrophages. J Virol [Internet]. 2019 Jun [cited 2025 Nov 12];93(12):e01436-19.
38. Acs B, Salgado R, Hartman J. What do we still need to learn on digitally assessed biomarkers? EBioMedicine [Internet]. 2021 Aug [cited 2025 Nov 12];70:103520.
39. Sun P, He J, Chao X, Chen K, Xu Y, Huang Q, et al. Computational tumor-infiltrating lymphocyte assessment method comparable with visual reporting guidelines for triple-negative breast cancer. EBioMedicine [Internet]. 2021 Aug [cited 2025 Nov 12];70:103492.